Influence of Linear Filters and Nonlinear Damping Models on the Stochastic Roll Response of a Ship in Random Seas

Wei Chai, *Department of Marine Technology,*

Norwegian University of Science and Technology chai.wei@ntnu.no

Arvid Naess, *Centre for Ships and Ocean Structures & Department of Mathematical Sciences,*

Norwegian University of Science and Technology arvid.naess@ntnu.no

Bernt J. Leira, *Department of Marine Technology,*

Norwegian University of Science and Technology bernt.leira@ntnu.no

ABSTRACT

Roll motion is the most critical ship motion leading to capsizing. The single-degree-of-freedom (SDOF) model is applied in order to simulate the roll motion in random beam seas. The random wave excitation term in the SDOF model is approximated by a second-order linear filter or more accurately, by a fourth-order linear filter as a filtered white noise process. Then the original SDOF model would be extended into a four-dimensional (4D) or a six-dimensional (6D) dynamic system, respectively. For the 4D coupled system, it can be viewed as a Markov system whose probability properties are governed by the corresponding Fokker-Planck equation. With the advantage of Markov property, the stochastic roll response can be obtained by the efficient 4D path integration (PI) method. The effect of different damping models, i.e. the linear-plus-quadratic damping (LPQD) model and linear-plus-cubic damping (LPCD) model, on the stochastic roll response is investigated. Furthermore, Monte Carlo simulation is introduced in order to validate the stochastic roll responses calculated by the 4D PI method as well as to study the influence of two different linear filter models on the response statistics.

KEYWORDS: *stochastic roll response; path integration method; filtering technique; nonlinear damping; Monte Carlo simulation.*

1. INTRODUCTION

For large amplitude roll motion in random seas, ship motion is strongly nonlinear and the dynamic behaviour of the vessel as well as the stochastic nature of random wave excitation should be taken into consideration in ship stability analysis. Moreover, the problem of estimating the stochastic response of nonlinear dynamic system excited by random external loads has been a demanding challenge for several decades (Naess & Johnsen, 1993).

Markov models have been widely applied in the area of stochastic dynamic analysis of roll motion in random seas. The shaping filter technique is introduced in order to approximate the wave excitation as a filtered white noise process. Subsequently, an augmented dynamic system is created when the original dynamic system is coupled with the filter model. Under the Markov theory, the joint probability density function (PDF) of the roll response can be obtained by solving the governing equation, i.e.

the Fokker-Planck (FP) equation. However, extended dynamic system usually corresponds to a high-dimensional FP equation and analytical solutions to high-dimensional FP equations are only available for some linear systems and a very restricted class of nonlinear systems.

The path integration (PI) method is an efficient approximation for solving the high-dimensional FP equations with reliable accuracy. This method is based on the Markov property of the dynamic system and the global solution of the FP equation can be constructed by linking the explicitly known local solutions. Recently, this algorithm was successfully extended to 4D for studying the stochastic roll response of a ship in random beam seas (Chai et al. 2014).

Besides the efficient PI method, Monte Carlo simulation is another methodology to determine the response statistics of the nonlinear dynamic systems subjected to random external forcing. The nonlinear and time-dependent terms can be easily and directly dealt with. However, the main drawback of Monte Carlo simulation is the associated computational efficiency will be sacrificed for estimation of the extreme responses with low probability levels.

The nonlinearity of the roll damping has been recognized to be crucial for evaluating the ship stability since Froude's time (Bikdash et al., 1994). Since the quantitative evaluation of roll damping is difficult, empirical models are used to describe the roll damping term. The linear-plus-quadratic damping (LPQD) model has been verified by numerous studies of experimental data (Roberts & Vasta, 2000). On the other hand, the linear-plus-cubic damping (LPCD) model is infinitely differentiable, and mathematically preferable to the LPQD model. Bikdash et al (1994) derived a condition under which the LPCD model approximates well with the LPQD model in a least-squares sense.

In this paper, the wave excitation spectrum is modelled by a second-order linear filter and a more precise fourth-order linear filter. The effect of different linear filters on the stochastic roll response is investigated by comparison with the Monte Carlo data. The LPQD model is transformed into a LPCD model by the least square method. Then, the influence of two different damping models on the stochastic roll response, especially on the extreme response are evaluated. The accuracy of the 4D PI method is verified by means of the versatile Monte Carlo simulation technique.

2. THEORETICAL BACKGROUND

2.1 Mathematical model of roll motion

When the ship is excited by beam wave loads, the rolling behaviour can be represented by the following single-degree-of-freedom (SDOF) equation:

$$(I_{44} + A_{44})\ddot{\theta}(t) + B_{44}\dot{\theta}(t) + B_{44q}\dot{\theta}(t)\left|\dot{\theta}(t)\right|$$
$$+ \Delta(C_1\theta(t) - C_3\theta^3(t)) = M(t) \qquad (1)$$

where $\theta(t)$ and $\dot{\theta}(t)$ are the roll angle and the roll velocity, respectively. I_{44} is the moment of inertia with respect to an axis through an assumed roll center, A_{44} denotes the added mass coefficient. B_{44} and B_{44q} are the linear and quadratic damping coefficients. Δ is the displacement of the vessel, C_1 and C_3 are the linear and nonlinear roll restoring coefficients of the restoring arm. $M(t)$ represents the random wave excitation moment.

The wave elevation and wave excitation moment are assumed to be stationary Gaussian stochastic processes. The wave excitation moment spectrum, $S_{MM}(\omega)$, can be determined as follows(Jiang et al., 1996):

$$S_{MM}(\omega) = \left|F_{roll}(\omega)\right|^2 S_{\zeta\zeta}(\omega) \qquad (2)$$

in which $S_{\zeta\zeta}(\omega)$ is the wave energy spectrum, $|F_{roll}(\omega)|$ represents the roll excitation moment amplitude per unit wave height.

Dividing equation (1) by $(I_{44} + A_{44})$, the final form of the differential equation is obtained as:

$$\ddot{\theta}(t) + b_{44}\dot{\theta}(t) + b_{44q}\dot{\theta}(t)\left|\dot{\theta}(t)\right| \tag{3}$$
$$+ c_1\theta(t) - c_3\theta^3(t) = m(t)$$

where b_{44}, b_{44q}, c_1 and c_3 are relative roll parameters. The spectrum of the relative roll excitation moment, $S_{mm}(\omega)$, is expressed as:

$$S_{mm}(\omega) = \left|F_{roll}(\omega)\right|^2 S_{\zeta\zeta}(\omega)\Big/(I_{44} + A_{44})^2 \tag{4}$$

Furthermore, the SDOF model (3) can be transformed into the following state-space equation:

$$\begin{cases} dx_1 = x_2 dt \\ dx_2 = (-b_{44}x_2 - b_{44q}x_2\left|x_2\right| - c_1x_1 + c_3x_1^3 + x_3)dt \end{cases} \tag{5}$$

where $x_1 = \theta(t)$, $x_2 = \dot{\theta}(t)$, $x_3 = m(t)$.

2.2 Shaping filter technique

Dostal and Kreuzer (2011) proposed a second-order and a fourth-order linear filter to fit the desired narrow-banded spectrum. In this work, both of the linear filters can be applied in order to model the target spectrum, i.e. the relative wave excitation moment spectrum $S_{mm}(\omega)$. The second-order linear filter is given by the following differential equation

$$\begin{cases} dx_3 = (x_4 - \beta x_3)dt + \gamma dW \\ dx_4 = -\alpha x_3 dt \end{cases} \tag{6}$$

where x_3 and x_4 are the state variables in the filter equation with x_3 representing the output $m(t)$. $dW(t)=W(t+dt)-W(t)$ is the increment of a Wiener process with $E\{dW(t)\}=0$ and $E\{dW(t) dW(t+dt)\}=\delta(dt)$, where $\delta(\cdot)$ represents the Dirac function. The spectrum generated by equation (6) is given by

$$S_{2nd}(\omega) = \frac{1}{2\pi}\frac{\gamma^2\omega^2}{(\alpha - \omega^2)^2 + (\beta\omega)^2} \tag{7}$$

The fourth-order linear filter which represents a more accurate approximation is given by the following expression:

$$\begin{cases} dx_5 = (x_6 - \lambda_1 x_5)dt \\ dx_6 = (x_7 - \lambda_2 x_5)dt + \gamma_1 dW \\ dx_7 = (x_8 - \lambda_3 x_5)dt \\ dx_8 = -\lambda_4 x_5 dt \end{cases} \tag{8}$$

where x_5, x_6, x_7, x_8 are variables introduced for the state-space representation and x_5 represents the filter output $m(t)$. The spectrum generated by equation (11) will have the following form:

$$S_{4th}(\omega) = \frac{1}{2\pi}\frac{\gamma_1^2\omega^4}{[(\beta_1 - \omega^2)^2 + (\alpha_1\omega)^2][(\beta_2 - \omega^2)^2 + (\alpha_2\omega)^2]} \tag{9}$$

where the parameters λ_1, λ_2, λ_3, λ_4 in equation (9) can be determined by the following relationship: $\lambda_1 = \alpha_1 + \alpha_2$, $\lambda_2 = \beta_1 + \beta_2 + \alpha_1\alpha_2$, $\lambda_3 = \alpha_1\beta_2 + \alpha_2\beta_1$, $\lambda_4 = \beta_1\beta_2$. The parameters α, β, γ in the second-order linear filter and the parameters α_1, α_2, β_1, β_2, γ_1 in the fourth-order filter are determined by a least-square algorithm which is utilized for fitting of the target spectrum, $S_{mm}(\omega)$. The bandwidth and the peak frequency of the filtered spectrum can easily be adjusted by changing the values of these parameters.

By combining the governing equation of the roll motion (5) with the linear filter equation (6) or (8), ship roll motion in random beam seas can be described by a 4D or a 6D state space equation, respectively.

2.3 Path integration method

The 4D state space equation can be expressed as follows:

$$\begin{cases} dx_1 = x_2 dt \\ dx_2 = (-b_{44}x_2 - b_{44q}x_2\left|x_2\right| - c_1x_1 + c_3x_1^3 + x_3)dt \\ dx_3 = (x_4 - \beta x_3)dt + \gamma dW \\ dx_4 = -\alpha x_3 dt \end{cases} \tag{10}$$

Equation (10) represents a Markov dynamic system driven by Gaussian white noise. It can be expressed as an *Itô* stochastic differential equation (SDE):

$$d\mathbf{x} = a(\mathbf{x},t)dt + b(t)d\mathbf{W}(t) \tag{11}$$

where $x(t)=(x_1(t),\dots,x_4(t))^{\mathrm{T}}$ is a 4D state space vector process, the vector $a(\mathbf{x},t)$ represents the drift term and $b(t)d\mathbf{W}(t)$ is the diffusive term. The vector $d\mathbf{W}(t)=\mathbf{W}(t+dt)-\mathbf{W}(t)$ denotes independent increments of a standard Wiener process.

The solution $\mathbf{x}(t)$ to equation (11) is a Markov process and its transition probability density (TPD), also known as the conditional PDF, $p(\mathbf{x},t|\mathbf{x}',t')$ satisfies the FP equation which is casted in the following form:

$$\frac{\partial}{\partial t} p(\mathbf{x},t \mid \mathbf{x}',t') = -\sum_{i=1}^{4} \frac{\partial}{\partial x_i} a_i(\mathbf{x},t) p(\mathbf{x},t \mid \mathbf{x}',t')$$
$$+ \frac{1}{2}\sum_{i=1}^{4}\sum_{j=1}^{4} \frac{\partial^2}{\partial x_i \partial x_j}(b(t)\cdot b^T(t))_{ij} p(\mathbf{x},t \mid \mathbf{x}',t') \tag{12}$$

Unlike direct numerical techniques, such as the finite-element method and the finite difference method, aiming to solve the FP equation (12) and obtain the TPD directly, the PI method captures the probabilistic evolution of the process $\mathbf{x}(t)$ by taking advantage of the Markov property of the dynamics system (11). In principle, the PI method is an approximation approach and the PDF of the process $\mathbf{x}(t)$ can be determined by the following basic equation:

$$p(\mathbf{x},t) = \int_{R^4} p(\mathbf{x},t \mid \mathbf{x}',t')p(\mathbf{x}',t')d\mathbf{x}' \tag{13}$$

where $d\mathbf{x}' = \prod_{i=1}^{4} dx_i'$.

Specifically, the value of the PDF at time t, $p(\mathbf{x},t)$, can be calculated by equation (13) with the value of previous PDF at time t' as well as the value of conditional PDF, $p(\mathbf{x},t|\mathbf{x}',t')$. For a numerical solution of the SDE (11), a time discrete approximation should be introduced. Naess and Moe (2000) proposed a fourth-order Runge-Kutta-Maruyama (RKM) discretization approximation:

$$\mathbf{x}(t) = \mathbf{x}(t') + r(\mathbf{x}(t'),t')\Delta t + b(t')\Delta\mathbf{W}(t') \tag{14}$$

where the vector $r(\mathbf{x}(t'),\ t')$ is the explicit fourth-order Runge-Kutta approximation or the Runge-Kutta increment. Since $\mathbf{W}(t)$ is a Wiener process, the independent increment $\Delta\mathbf{W}(t')=\mathbf{W}(t)-\mathbf{W}(t')$ is a Gaussian variable for every t'.

If we consider only the deterministic part of equation (11), the approximation (14) reduces to the fourth-order Runge-Kutta approximation $\mathbf{x}(t)=\mathbf{x}(t')+r(\mathbf{x}(t'),t')\Delta t$. Experiments have shown that, for the Markov systems, the accuracy associated with approximating the deterministic terms is the most important (Mo, 2008). In this regard, the accuracy of the fourth-order RKM approximation is satisfactory since the fourth-order Runge-Kutta approximation follows the time evolution of the deterministic part of equation (11) with an accuracy to the order of $O(\Delta t^5)$.

The time sequence $\{\mathbf{x}(i\cdot\Delta t)\}_{i=0}^{\infty}$ is a Markov chain and it can approximate the time-continuous Markov process solution of the SDE (11) when the time increment $\Delta t=t-t'$ is sufficiently small. Moreover, the conditional PDF of the process x(t), $p(\mathbf{x},t|\mathbf{x}',t')$, follows a (degenerate) Gaussian distribution and it can be written as (Naess & Johnsen, 1993):

$$p(\mathbf{x},t \mid \mathbf{x}',t') = \delta(x_1 - x_1' - r_1(\mathbf{x}',\Delta t))$$
$$\cdot \delta(x_2 - x_2' - r_2(\mathbf{x}',\Delta t))\cdot \tilde{p}(x_3,t \mid x_3',t') \tag{15}$$
$$\cdot \delta(x_4 - x_4' - r_4(\mathbf{x}',\Delta t))$$

where $\tilde{p}(x_3,t \mid x_3',t')$ is given by the relation:

$$\tilde{p}(x_3,t \mid x_3',t') = \frac{1}{\sqrt{2\pi\gamma^2\Delta t}}$$
$$\cdot \exp\left\{-\frac{(x_3 - x_3' - r_3(\mathbf{x}',\Delta t))^2}{2\gamma^2\Delta t}\right\} \tag{16}$$

in which $r_i(\mathbf{x}',\ \Delta t)$, i=1,2,3,4, are the Runge-Kutta increments for the state space variables.

Since the expression for the conditional PDF is known, the time evolution of the PDF of $\mathbf{x}(t)$ can be determined by the iterative algorithm (17) if an initial PDF $p(\mathbf{x}^{(0)}, t_0)$ is given

$$p(\mathbf{x},t) = \int_{R^4} \cdots \int_{R^4} \prod_{i=1}^{n} p(\mathbf{x}^{(i)},t_i \mid \mathbf{x}^{(i-1)},t_{i-1}) \\ \cdot p(\mathbf{x}^{(0)},t_0)d\mathbf{x}^{(0)}\ldots d\mathbf{x}^{(n-1)} \quad (17)$$

where $\mathbf{x} = \mathbf{x}^{(n)}$, $t = t_n = t_0 + n \cdot \Delta t$.

Equation (17) describes the mathematical principle of the PI approach. In this work, the initial PDF $p(\mathbf{x}^{(0)}, t_0)$ is chosen as a 4D Gaussian PDF with zero mean and variances evaluated by a simple Monte Carlo simulation. The straightforward Monte Carlo simulation ensures that the initial 4D Gaussian PDF includes all the information corresponding to the selected parameters of the dynamic system, and it also provides a rational computational domain for the subsequent simulation. For the numerical implementation of the iterative algorithm (17), it represents the PDF at the previous time t' as an interpolating spline surface via parabolic B-spline and then it evaluates the PDF at time t by several specific steps. The numerical iterative algorithm and the associated specific computational steps have been systematically described by Iourtchenko et al (2006) and Yurchenko et al (2013). Moreover, the capability of the PI method in producing accurate and reliable solutions for the stochastic dynamic systems has been demonstrated by numerous examples (Mo, 2008).

3. MEAN UPCROSSING RATE

The mean upcrossing rate is a key parameter for estimating the stochastic responses, especially the large and extreme responses. A nice aspect of the PI method is that the joint PDF of the roll angle and the roll velocity can be calculated directly. Then the mean upcrossing rate can be given by the Rice formula

$$v^+(\zeta;t) = \int_0^{\infty} \dot{\theta} f_{\theta\dot{\theta}}(\zeta,\dot{\theta};t)d\dot{\theta} \quad (18)$$

where $v^+(\zeta;t)$ denotes the expected number of upcrossing for the ζ-level per unit time at time t by the roll angle $\theta(t)$, $f_{\theta\dot{\theta}}(\theta,\dot{\theta};t)$ is the joint PDF of the roll angle and the roll velocity at the time instant t.

For nonlinear ship rolling in beam seas, due to the presence of negative nonlinear stiffness term in the SDOF model (1), ship capsizing may happen when the predetermined simulation time T is long enough or the intensity of the external excitation is strong enough. If the mean time to capsize is long enough, the dynamic system can be regarded as a highly reliable system and the corresponding roll response reaches stationarity in an approximate sense (Roberts & Vasta, 2000).

As for the four-dimensional dynamic system (10) or the six-dimensional dynamic system obtained by combing the equations (5) and (8), the fourth-order RKM method is adopted to solve the corresponding SDE. The mean upcrossing rates can be estimated from the time series of responses. Let $n_i^+(\xi;T_i)$ denote the counted number of upcrossing for the level ζ during the time interval $(0, T_i)$ for simulated time history No. i. The appropriate sample mean value of averaged mean upcrossing rate, $\hat{v}^+(\xi)$ is then obtained as:

$$\hat{v}^+(\zeta) = \frac{\sum_{i=1}^{k} n_i^+(\zeta;T_i)}{\sum_{i=1}^{k} T_i} \quad (19)$$

A fair approximation of the 95% confidence interval, $CI_{0.95}$, for the value of $\hat{v}^+(\xi)$ can be obtained as (Naess et al, 2007):

$$CI_{0.95}(\zeta) = \left(\hat{v}^+(\zeta) - 1.96\frac{\hat{s}(\zeta)}{\sqrt{k}}, \hat{v}^+(\zeta) + 1.96\frac{\hat{s}(\zeta)}{\sqrt{k}} \right) \quad (20)$$

Where the empirical standard deviation $\hat{s}(\xi)$ is given as

$$\hat{s}(\zeta)^2 = \frac{1}{k-1} \sum_{i=1}^{k} \left(\frac{n_i^+(\zeta;T_i)}{T_i} - \hat{v}^+(\zeta) \right)^2 \qquad (21)$$

Moreover, the selection of the number of simulation, k, for the Monte Carlo simulation is selected according to the upcrossing rates in the tail region and the length of the predetermined simulation time T. Usually, low upcrossing rates and short time periods T corresponds to a large simulation number k.

Ship stability failure occurs when the roll angle exceeds some certain values, such as the angle of vanishing stability or some large roll angle leading to damage. Assume that the upcrossing events in the high level response region are statistically independent and the random process $\theta(t)$ is not extremely narrow-banded, the exceedance probability for a duration of exposure time T, $P_\Theta(T)$, can be approximated by a widely used Poisson estimate, which is given as follows:

$$\begin{aligned} P_\Theta(T) &= 1 - \exp(-\int_0^T v^+(\zeta;t)dt) \\ &\approx 1 - \exp(-v^+(\zeta) \cdot T) \end{aligned} \qquad (22)$$

where $v^+(\zeta)$ represents the mean upcrossing rate of the level ζ at a suitable reference point in time, which can be determined directly by the 4D PI approach and the Rice formula (18).

4. SIMULATION RESULTS

4.1 Ship parameters and excitation spectrum

In this section, an ocean surveillance ship (Su, 2012), is selected for studying the stochastic responses of ship rolling. The parameters of the vessel and the natural roll frequency, ω_0, are given in Table 1.

The modified P-M spectrum, widely used for the fully developed ocean waves, is adopted in this analysis.

$$S_{\xi\xi}(\omega) = \frac{5.058g^2 H_s^2}{T_p^4 \omega^5} \exp(-1.25 \frac{\omega_p^4}{\omega^4}) \qquad (23)$$

in which H_s denotes the significant wave height, ω_p is the peak frequency at which the wave spectrum $S_{\xi\xi}(\omega)$ has its maximum, and T_p is the corresponding peak period.

Table 1   List of parameters for the vessel

Parameters	Dimensional value
$I_{44}+A_{44}$	5.540×10^7 kg·m^2
B_{44}	5.266×10^6 kg·m^2·s^{-1}
B_{44q}	2.877×10^6 kg·m^2
Δ	2.017×10^7 N
C_1	3.168 m
C_3	2.513 m
ω_0	1.074 rad/s

Three different sea states, i.e. different external excitations, are selected for analyzing the stochastic roll responses. The wave spectra and rolling excitation moment amplitude per unit wave height of the vessel are plotted in Figure 1.

The parameters α, β, γ in the second-order filter (6) and parameters λ_1, λ_2, λ_3, λ_4 in the fourth-order filter (8) can be determined by the least square scheme which is available in the curve fitting algorithms of MATLAB. The parameters in these two linear filters for different sea states are presented in Tables 2 and 3. Moreover, the fitting results of the relative wave excitation spectrum for sea state 1 are shown in Figure 2.
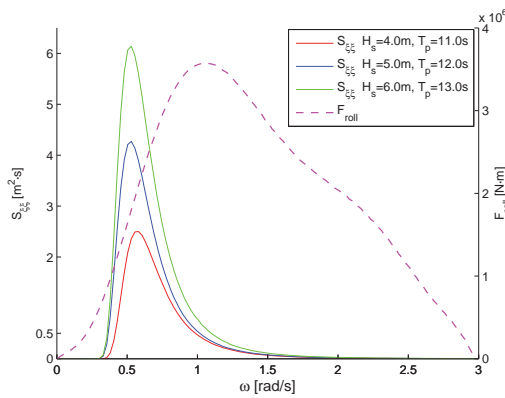
Figure 1   Wave spectra for different sea states and rolling excitation moment amplitude per unit wave height

Table 2   Parameters of the second-order linear filter for different sea states

Sea States	H_s (m)	T_p (s)	α	β	γ
Sea state 1	4.0	11.0	0.495	0.366	0.0432
Sea state 2	5.0	12.0	0.441	0.364	0.0498
Sea state 3	6.0	13.0	0.390	0.365	0.0555

Table 3   Parameters of the fourth-order linear filter for different sea states

H_s (m)	T_p (s)	λ_1	λ_2	λ_3	λ_4	γ_1
4.0	11.0	0.934	1.431	0.486	0.310	0.0363
5.0	12.0	0.924	1.309	0.429	0.249	0.0414
6.0	13.0	0.931	1.212	0.390	0.202	0.0461
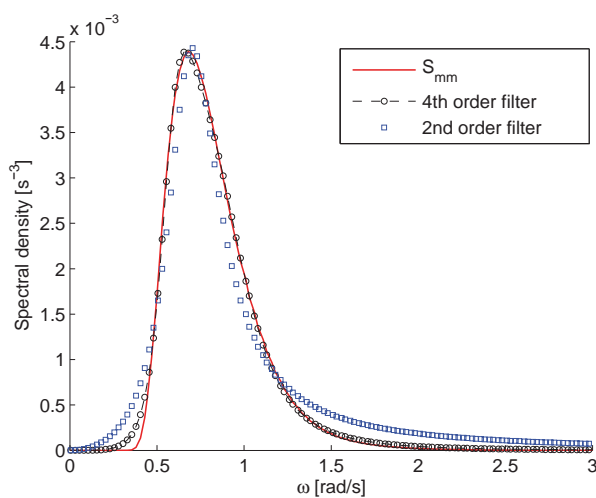
Figure 2   Relative wave excitation spectrum in equation (4) and filtered spectra for sea state 1

4.2   Influence of linear filter

The transfer function between wave excitation and roll response in the SDOF model (1) is narrow-banded due to the light roll damping. Thus, the fitting accuracy near the natural roll frequency, ω_0, has a significant effect on the subsequent rolling responses. However, there is a slight discrepancy between the spectral density generated by the second-order filter and the target spectral density in Figure 2. Therefore, a constant, c, should be introduced as a correction factor for the filtered spectral density to decrease the discrepancy in the critical region near roll frequency ω_0. The filtered spectrum (12) can be changed to:

$$S_{2nd}(\omega) = \frac{1}{2\pi} \frac{(c \cdot \gamma)^2 \omega^2}{(\beta - \omega^2)^2 + (\alpha\omega)^2} \qquad (24)$$

The correction factor c is taken to be 1.07 by considering the mean difference of the two spectral densities in the critical frequency region. As mentioned in section 3, the joint probability density function (PDF) of the roll angle and the roll velocity can be obtained directly by the 4D PI method. The joint PDF of the roll response for sea state 1 is presented in Figure 3, while Figure 4 displays the contour lines of the joint PDF.
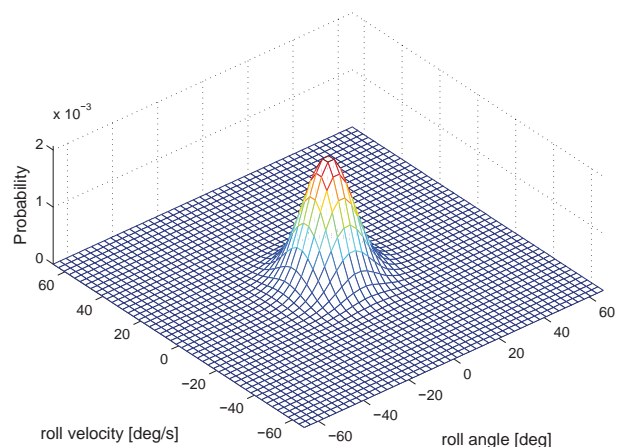

Figure 3   Joint PDF of the roll response for sea state 1 with H_s=4.0m, T_p=11.0s
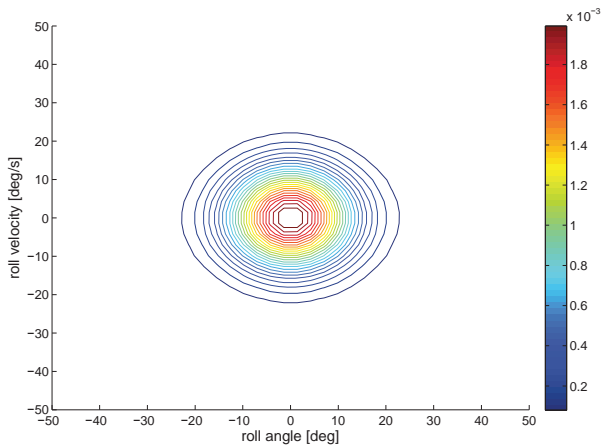
Figure 4 Contour lines of the joint PDF of the roll response for sea state 1

It can be observed in Figures 3 and 4 that the PDF of the roll response is symmetric. This is reasonable since the distribution of the random wave excitation, i.e. the filtered white noise process, and the vessel properties are symmetric with respect to the origin. Moreover, the marginal PDF of the roll angle process and the marginal PDF of the roll velocity process obtained by the 4D PI method and the 4D Monte Carlo simulation are plotted in Figure 5 and 6, respectively.
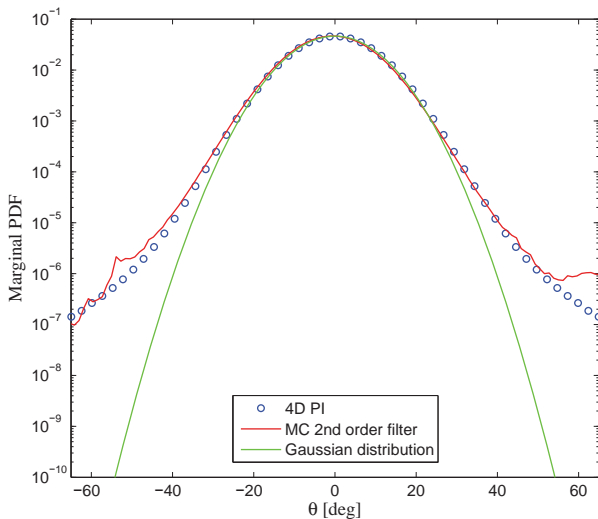
Figure 5 Marginal PDF of the roll angle process for sea state 1
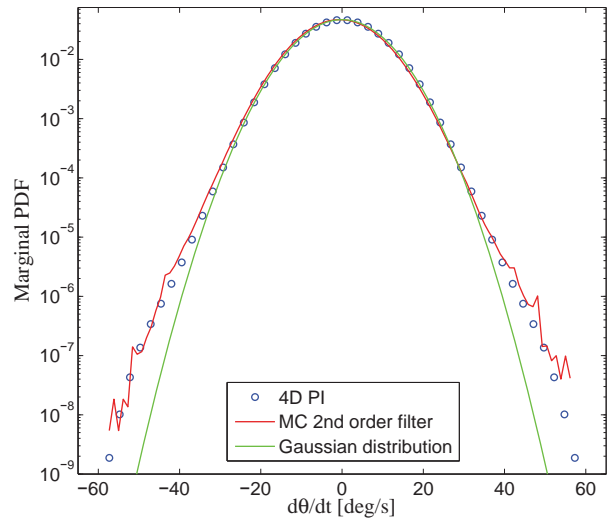
Figure 6 Marginal PDF of the roll velocity process for sea state 1

It is shown in Figures 5 and 6 that the Gaussian distribution gives a reasonable approximation of the statistics of small-amplitude roll motions. However, for the high-level responses, Gaussian distribution under-estimates the corresponding low probability levels in this region. Moreover, the 4D PI method provides nice results for the low probabilities, where the distributions obtained by the versatile Monte Carlo simulation are suffering from uncertainties.

The importance of the correction factor c for the stochastic roll response is illustrated in Figure 7. It can be observed that, the slight discrepancy between the second-order filtered spectrum and the target spectrum in the critical region, which is shown in Figure 2, results in noticeable influence on the subsequent roll response. If there is no correction factor for the second order linear filter, the stochastic roll response, will be significantly underestimated. In addition, the good agreement of the upcrossing rates obtained by 4D PI method and 6D Monte Carlo simulation (MCS) verify the rationality of the correction factor.
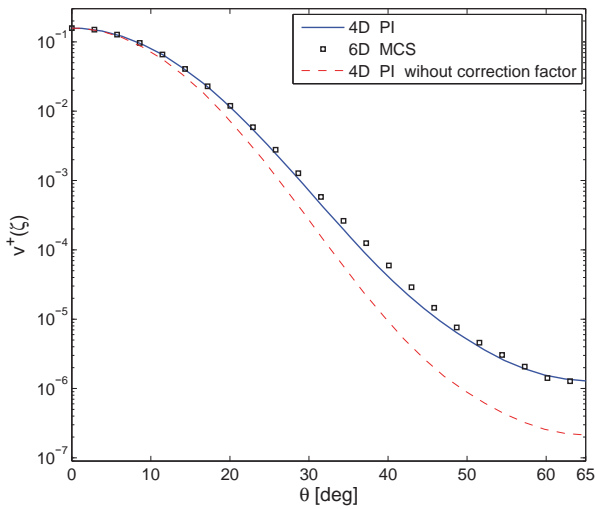
Figure 7   Influence of the correction factor, c, on the upcrossing rate for sea state 1 with H_s=4.0m, T_p=11.0s

The comparisons between the upcrossing rates calculated by the 4D PI method and the empirical estimation of the upcrossing rates as well as the 95% confidence intervals obtained by 4D Monte Carlo simulations for different sea states can be viewed in Figures 8, 9 and 10. It can be readily seen that the 4D PI approach yields accurate and reliable results for various external excitation cases. Next, the empirical estimation of the upcrossing rates computed by 6D Monte Carlo simulations are plotted in these Figures. The good agreement of the 4D results and 6D results extracted from Monte Carlo simulation verify the rationality of introducing the correction factor for all of the cases.
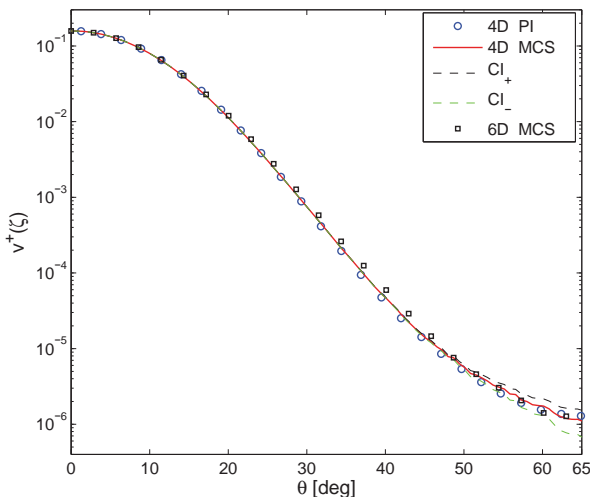
Figure 8   Upcrossing rate for sea state 1 with

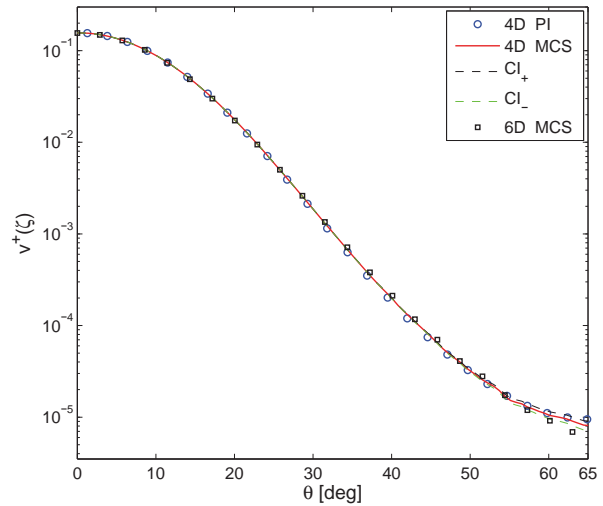H_s=4.0m, T_p=11.0s (simulation number k =3000)

Figure 9   Upcrossing rate for sea state 2 with H_s=5.0m, T_p=12.0s (simulation number k = 1500)
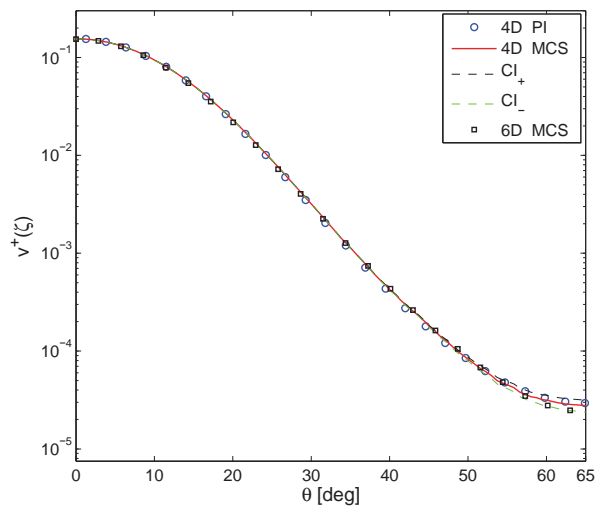

Figure 10   Upcrossing rate for sea state 3 with H_s=6.0m, T_p=13.0s (simulation number k = 1000)

4.3   Influence of nonlinear damping models

The roll damping is mainly due to three different sources: the free surface radiated wave damping, the damping caused by vortex shedding and flow separation and finally the

viscous friction damping. In general, these damping terms are coupled with each other. The linear-plus-quadratic damping (LPQD) model is one of the most common expressions used in the SDOF equation (1). This model is given as:

$$b_{44}\dot{\theta}(t) + b_{44q}\dot{\theta}(t)\left|\dot{\theta}(t)\right| \tag{25}$$

However, the LPQD model is only once continuously differentiable and mathematically inferior to the infinitely differentiable linear-plus-cubic damping (LPCD) model. The LPCD model is written as:

$$b'_{44}\dot{\theta}(t) + b_{44c}\dot{\theta}^3(t) \tag{26}$$

The least square method is a typical approach used to transform the LPQD model into the LPCD model. The result of fitting the two damping models is shown in Figure 11. Moreover, the roll response spectra for the dynamic systems with different damping models for sea state 1 are plotted in Figure 12.
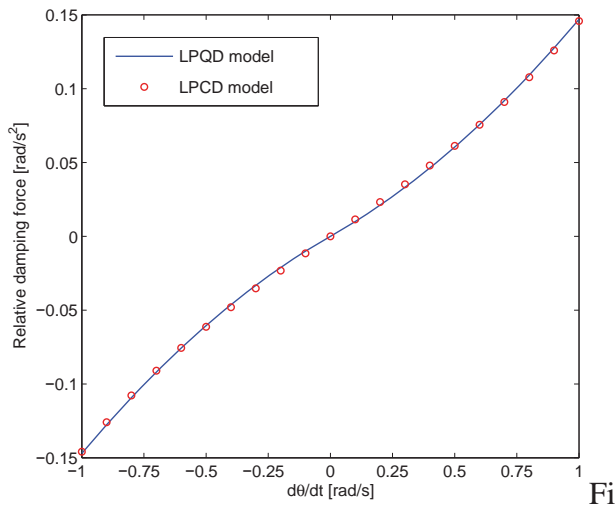

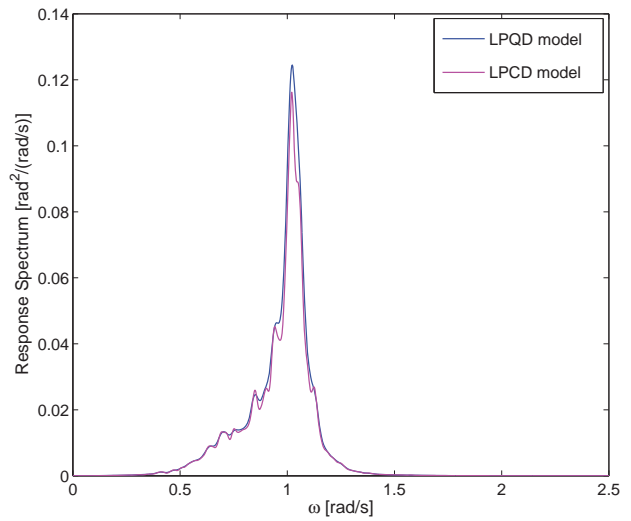gure 11   Fitting result for the LPQD and LPCD models

Figure 12   Roll response spectra for the LPQD and LPCD models for sea state 1

It is illustrated in Figure 11 that the two damping models have a good agreement in the least-square sense. Nevertheless, in Figure 12, there is still a slight discrepancy between the response spectra in the peak region, i.e. the critical frequency region near natural roll frequency ω_0. The upcrossing rates, obtained by the 4D PI method and the 4D Monte Carlo simulation, for the LPQD model versus the LPCD model for different sea states are plotted in Figures 13, 14 and 15, respectively.
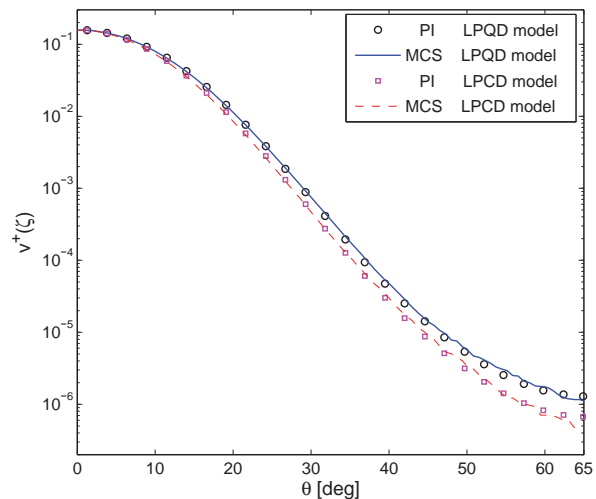

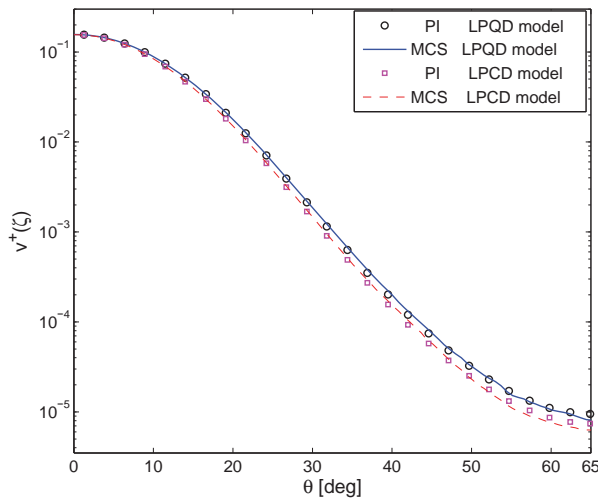Figure 13   Upcrossing rate for different damping models for sea state 1

Figure 14   Upcrossing rate for different damping models for sea state 2

Figure 15 Upcrossing rate for different damping models for sea state 3

The 4D PI approach is available to provide high-accuracy results for both models when compared with the corresponding empirical estimations obtained by 4D Monte Carlo simulations. However, the corresponding upcrossing rates under the same sea sate are quite different, even though the two damping models match well in the least-square sense. The discrepancies between the upcrossing rates in the tail regions, suggest that the LPCD model might underestimate the extreme response of the dynamic system. Therefore, the traditional least square method, applied to transform the LPQD model into the LPCD model, cannot guarantee the accuracy of the subsequent stochastic roll response. Furthermore, from the observations in Figures 13-15, it can be predicted that when the stochastic linearization technique is applied in order to linearize the nonlinear damping term (25), even more significant discrepancy of the upcrossing rate would be observed in the tail region.
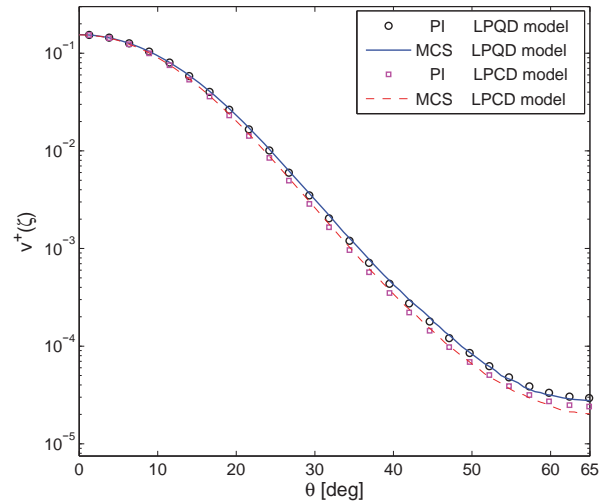
5.   CONCLUSIONS

In this paper, the 4D path integration technique and Monte Carlo simulation were applied in order to investigate the influences of linear filter models and nonlinear damping models on the stochastic roll response of a vessel in random beam seas. From the numerical results and discussions above, some of the results can be summarized:

The correction factor, c, is important and reasonable to be introduced into the second-order linear filter. Moreover, the accuracy of the filtered spectrum in the critical frequency region is crucial for prediction of the response statistical. The 6D dynamic system can be simplified as a corresponding 4D dynamic system with a modified second-order linear filter due to the high-accuracy agreements for the upcrossing rates.

The typical least square method results in an underestimation of the upcrossing rate when it is used to transform a LPQD model into a LPCD model. The discrepancies between the upcrossing rates generated by different damping models should not be ignored.

It has been shown that the 4D PI approach yields reliable results for different damping

models and various excitation cases, even in the tail regions with low probability levels. Therefore, the 4D PI technique can be applied for the stochastic analysis of nonlinear ship rolling in random beam seas.

6. ACKNOWLEDMENTS

7. REFERENCES

Bikdash, M., Balachandran, B., Navfeh, A., 1994, "Melnikov analysis for a ship with a general roll-damping model", Nonlinear Dynamics, Vol. 6, pp. 101-124.

Chai, W., Naess, A., Leira, B. J., 2014, "Stochastic dynamic analysis of nonlinear ship rolling in random beam seas", Proceeding of the 7th International Conference on Computational Stochastic Mechanics, in press.

Dostal, L., Kreuzer, E., 2011, "Probabilistic approach to large amplitude ship rolling in random seas", Proceedings of the Institution of Mechanical Engineers, Part C: Journal of Mechanical Engineering Science, Vol. 225, pp. 2464-2476.

Iourtchenko, D.V., Mo, E., Naess, A., 2006, "Response probability density functions of strongly non-linear systems by the path integration method", International Journal of Non-Linear Mechanics, Vol. 41, pp. 693-705.

Jiang, C., Troesch, A.W., Shaw, S., 1996, "Highly nonlinear rolling motion of biased ships in random beam seas", Journal of ship research, Vol. 40, pp. 125-135.

Mo, E., 2008, "Nonlinear stochastic dynamics and chaos by numerical path integration", Ph.D. Thesis, Norwegian University of Science and Technology, Trondheim, Norway.

Naess, A., J. Johnsen, 1993, "Response statistics of nonlinear, compliant offshore structures by the path integral solution method", Probabilistic Engineering Mechanics, Vol. 8, pp. 91-106.

Naess, A., Gaidai, O., Teigen, P.S., 2007, "Extreme response prediction for nonlinear floating offshore structures by Monte Carlo simulation", Applied Ocean Research, Vol. 29, pp. 221-230.

Naess, A., Moe, V., 2000, "Efficient path integration methods for nonlinear dynamic systems", Probabilistic Engineering Mechanics, Vol. 15, pp. 221-231.

Roberts, J. and Vasta, M., 2000, "Markov modelling and stochastic identification for nonlinear ship rolling in random waves", Philosophical Transactions of the Royal Society of London. Series A: Mathematical, Physical and Engineering Sciences, Vol. 358, pp. 1917-1941.

Su, Z., 2012, "Nonlinear response and stability analysis of vessel rolling motion in random waves using stochastic dynamical systems", Ph.D. Thesis, Texas A & M University, Texas.

Yurchenko, D., Naess, A., Alevras P., 2013, "Pendulum's rotational motion governed by a stochastic Mathieu equation", Probabilistic Engineering Mechanics, Vol. 31, pp. 12-18.